11TH EUROPEAN
ADAMS USERS' CONFERENCE
Frankfurt - November 1996

COMPARISON OF ADAMS™ RAIL RESULTS WITH EUROPEAN BENCHMARK DATA

A. GUGLIOTTA, A. SOMA'

Dipartimento di Meccanica
Politecnico di Torino
Cso. Duca degli Abruzzi 24 - 10129 Torino - Italy

KEYWORDS: rail, dynamic, contact, multibody

ABSTRACT

In the present paper stability analysis and high speed transient simulation of a railway vehicle has been studied. The system has been modelled by using the rail oriented module of the multibody computer code ADAMS. Different wheel-rail contact theories have been compared. At first an analysis according to the numerical benchmark proposed by the European Rail Research Institute has been performed in order to check the model. Thereafter the transient simulation is studied to evaluate the combined effect of non-linear contact and measured track irregularities.

INTRODUCTION

The requirement to increase the speed of a railway vehicle may induce vibrations and vehicle instability; as a consequence at minimum this leads to comfort reduction. In the field of railway applications multibody computers codes are used as tools to investigate whole vehicle dynamic, pantograph dynamic, noise reduction [1,2].

In the present work the dynamic of a railway vehicle is studied including different wheel-rail contact models in order to evaluate the critical speed [3] and the track irregularities interactions in transient simulations.

During the last decades several wheel-rail contact theories have been evolved and widely used in railway dynamic simulation. An excellent survey of wheel-rail rolling contact theories has been given by Kalker [4]. In the present paper different levels of wheel-rail contact have been taken into account introducing first the linear Kalker model and, as second step, the non-linear Kalker model [5-6].

A mathematical model for the simulation of the interaction between train, track and supporting structure has been made by using a new module, oriented to the rail vehicle

simulation, of the multibody simulation code ADAMS [7,8]. It is possible to define a user track layout taking into account the track irregularities, to model the vehicle introducing the effect of body flexibility and the non linear formulation of the contact.

As far as the code allows the possibility to write user subroutines, in the present work an automatic procedure for critical speed evaluation has been developed. At first the modal analysis solution allows to perform the extraction of the critical speed. In the second part the transitory analysis is performed. The analysis has been compared taking into account both the effect of wheel-rail contact and track irregularities.

SYMBOLS

a/b	contact area semiaxes	ξ_x	longitudinal creepage
$\mathbf{h} = (h_{nx}, h_{ny}, h_{nz})$	linear velocity of n-th body	ξ_y	lateral creepage
$\mathbf{W} = (W_{nx}, W_{ny}, W_{nz})$	angular velocity	ξ_{sp}	spin creepage
V	forward rolling velocity	F_{cx}	longitudinal creep force
$\mathbf{R} = (R_{nx}, R_{ny}, R_{ny})$	principal radii of curvature	F_{cy}	lateral creep force

MATHEMATICAL MODEL OF WHEEL-RAIL CONTACT

In fig. 1 a general scheme of wheel-rail contact is given. The dynamic behaviour of a railway vehicle is significantly affected by the interactive forces between the wheel and rail.

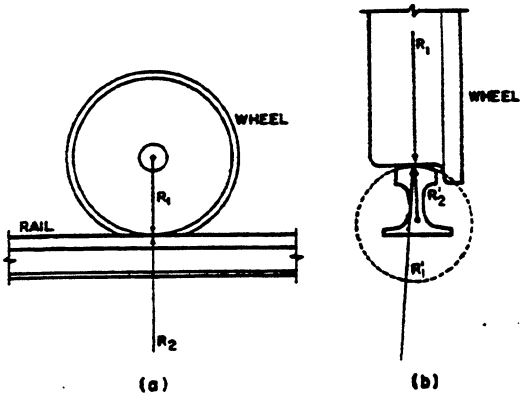

Fig. 1: wheel-rail contact scheme

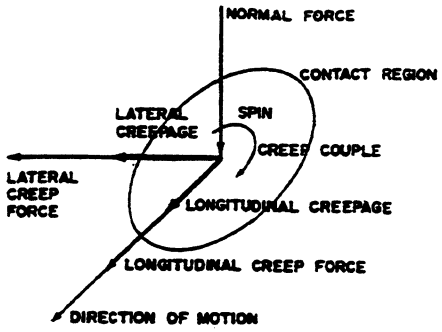

Fig. 2: contact forces scheme

These forces depends on the adhesion and creep. The phenomena of creep exist when two elastic bodies are pressed against each other with force and allowed to roll ever each other in presence of friction. A contact region is formed at the point at which they touch (fig. 2).

Several wheel-rail rolling contact theories have been evolved. Basically the theories may be divided in linear and non linear. The linear simplified theories starting from two dimensional Carter's theory (1926) to recent three dimensional Kalker theory (1967) [5] calculate the creep forces with a constant contact area. The non linear theories [6] take into account the variation of the contact area due to the different principal radii of curvature of the bodies of revolution during rolling.

A complete three dimensional non linear exact theories is given by Kalker [6] based on a minimum principle that satisfy the Coulomb inequality. Approximated non linear theory has been given by Kalker and may be used in numerical codes with the aids of numerical tables [9].

In a general case, from a kinematics point of view, creep occurs when the circumferential velocities of the two rolling bodies are not equal. The nondimensional term creepage is used to define these deviation from a pure rolling motion of the two bodies. The creepage are defined as follow:

- longitudinal creepage:

$$\xi_x = \frac{\left(h_{1x} - h_{2x} - R_{1x} \cdot W_{1y} - R_{2x} \cdot W_{2y}\right)}{V} = \frac{\text{actual forward velocity - pure rolling forward velocity}}{\text{forward velocity due to rolling}}$$

- lateral creepage:

$$\xi_y = \frac{h_{1y} - h_{2y}}{V} + \left(\frac{W_{1x}}{W_{1y}} - \frac{W_{2x}}{W_{2y}}\right) = \frac{\text{actual lateral velocity - pure rolling lateral velocity}}{\text{forward velocity due to rolling}}$$

- spin creepage:

$$\xi_{sp} = \frac{\left(W_{1z} - W_{2z}\right)}{V} = \frac{\text{angular velocity of upper body - angular velocity of lower body}}{\text{forward velocity due to rolling}}$$

The creep forces depends on the normal force trough the Coulomb inequality. According to Hertz static theory the contact region is elliptical and the ratio of the semiaxes (*a/b*) can be calculated from the principal radii of curvature of the bodies at the contact point. The calculation of the actual dimension *a* and *b* depends from the normal force. The area of contact will be divided as in scheme of fig. (3a) in a slip region and adhesion region. This influences the creep force/creepage relation in a non linear mode as schematically described in fig. (3b).

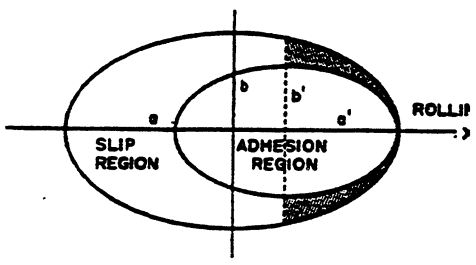

Fig 3a: slip and adhesion contact zone of the contact area

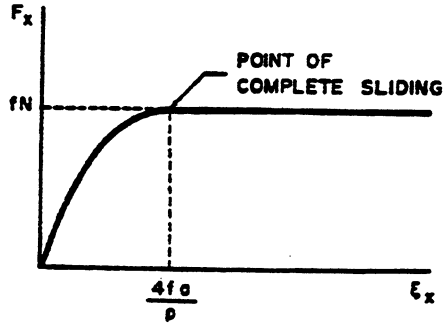

Fig 3b: creep force/creepage non linear function

In a general case the non-linear three dimensional rolling contact creep forces are derived as follows:

$$F_{cx} = -c(y)^2 \cdot G \cdot C(y)_{11} \cdot \xi_x$$
$$F_{cy} = -c(y)^2 \cdot G \cdot C(y)_{22} \cdot \xi_y \qquad (2)$$

$$Mz = -c(y)^3 \cdot G \cdot C(y)_{32} \cdot \xi_y - c(y)^4 \cdot G \cdot C(y)_{33} \cdot \xi_z$$

Where the semiaxes (*a/b*) of the contact area and the *C* coefficients may be calculated at each equilibrium position. In the linearized case the contact forces coefficients depends in a linear mode trough the kinematics creepage and equation is simplified as follows, where f_{ij} are called Kalker's coefficients:

$$\begin{aligned} F_{cx} &= -f_{11} \cdot \xi_x \\ F_{cy} &= -f_{22} \cdot \xi_y \\ Mz &= -f_{32} \cdot \xi_y - f_{33} \cdot \xi_z \end{aligned} \qquad (3)$$

NUMERICAL MODEL

The dynamic simulation of a railway vehicle leads to the a set of non linear equations. In order to perform the simulation of the vehicle multibody computer codes are used. In the present paper has been investigated the performance of the rail module of the ADAMS moltybody code.

The vehicle model used represent a European benchmark proposed by ERRI (European Rail Research Institute) as tool for computer code improvements [10]. The proposed vehicle is the Eurofima wagon and the basic data are listen in Table I.

Table I: mass and stiffness data of the vehicle Eurofima [10]

wagon mass	32000	[kg]	wagon total length	21.5	[m]
boogie mass	2600	[kg]	primary suspension stiffness	617	[KN/m]
wheelset mass	1500	[kg]	secondary suspension stiffness	160	[KN/m]

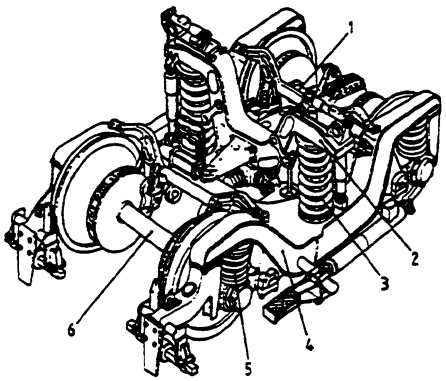

Fig. 4a: scheme of the Eurofima bogie: 1-engine wheelset; 2- support beam; 3-secondary suspension; 4- boogie; 5- primary suspension; 6- wheelset

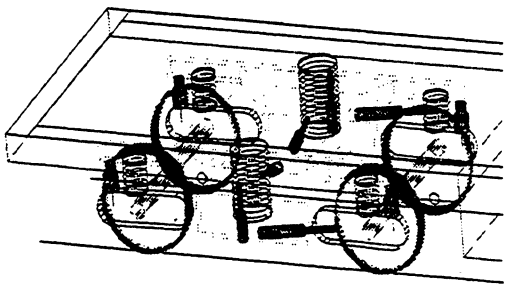

Fig. 4b: ADAMS model of the bogie

Fig. 4 shows a view of Eurofima boogie (a) and the ADAMS model scheme (b). The ADAMS View graphical simulation module allows the user to obtain a model closed to the design scheme. Therefore the debug operations of the model is helped with a powerful graphical interface.

MODAL DATA AND CRITICAL SPEED

In a first part of the work the numerical model is used to perform a comparison in terms of mode shape and frequencies between the benchmarks ERRI data and the results obtained with ADAMS and linearized wheel-rail contact theory. (Table II)

Table II: mode shape description and frequencies comparison between present model and ERRI benchmark models.

Mode description	ERRI Benchmark	ADAMS Rail
wagon lateral mode	0.47	0.55
yaw wagon	0.87	0.81
bounce wagon	1.16	1.10
pitch wagon	1.61	1.41
wagon vertical mode	1.55	1.36
1° wheelset yaw	2.23	2.38
2° wheelset yaw	2.27	2.438
bounce bogie (in phase)	6.34	6.42
bounce bogie (out phase.)	6.07	6.16
pitch bogie (in phase)	9.75	9.06
pitch bogie(out phase)]	9.74	9.07

The linear model has been also used in order to perform the stability analysis and the evaluation of the vehicle critical speed. For this specific goal a user subroutine has been written for the automatic critical speed vehicle identification. The critical speed comparison are listed in Table III.

Table III: critical speed comparison

	ERRI benchmark	ADAMS Rail
with non linear dampers	295 [Km/h]	311[Km/h]
with anti - yaw dampers	334 [Km/h]	342[Km/h]

TRANSIENT SIMULATION RESULTS

The transient simulation have been done by using a straight railway. The track is first modelled by using an analytical description.

Thereafter the track layout has been defined taking into account the effect of measured irregularities. The measured data are written in the code by using an input files data with the track co-ordinates and the cant angle for discrete points.

Table IV: summary of simulation cases

analytical/measured track	linear Kalker contact	non linear Kalker contact
no dampers	wagon lateral displ. (fig.6a) wheelset lateral displ. (fig. 7a)	wagon lateral displ. (fig.6b) wheelset lateral displ. (fig. 7b)
non-linear dampers	wagon lateral displ. (fig. 6c) wheelset lateral displ. (fig. 7c)	wagon lateral displ. (fig.6d) wheelset lateral displ. (fig. 7d)

The simulation correspond to a run with 250 km/h speed of a duration of 5 sec and about 230 m length selected from the measured track data given by the ERRI benchmark. Different simulations have been performed, as described in Table IV, taking into account linear and non linear wheel-rail contact theories and linear and non-linear dampers. In the graphs fig. 6-abcd the y displacement of the wagon are reported.

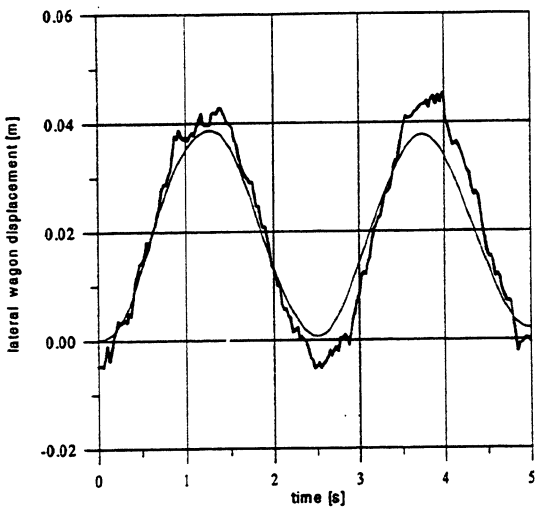

a) case with no dampers and linearized Kalker's contact

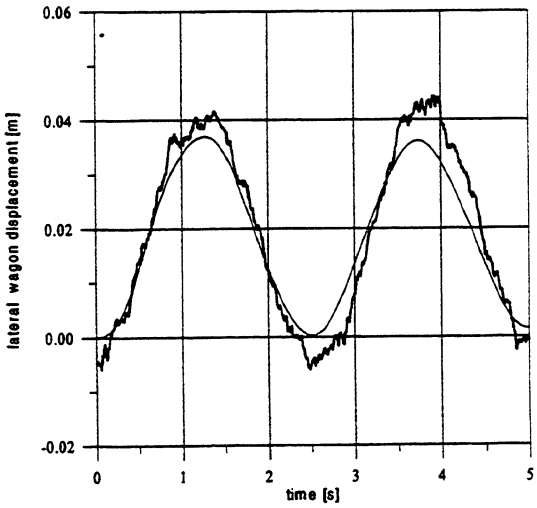

b) case with no dampers and non linear Kalker's contact

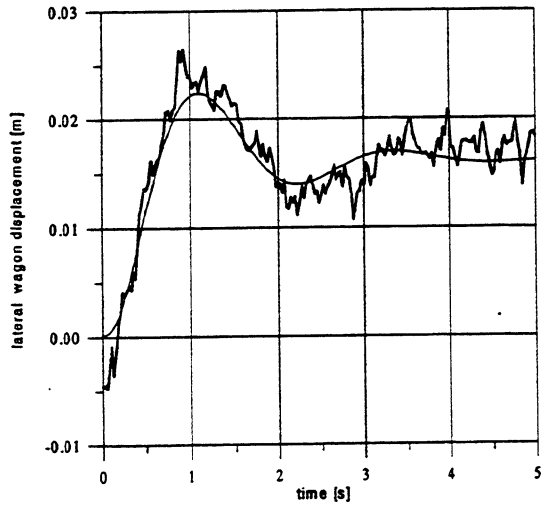

c) case with non linear dampers and linearized Kalker's contact

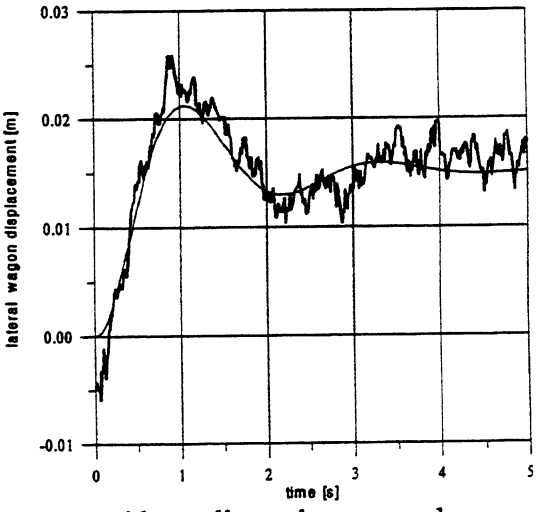

d) case with non linear dampers and non linear Kalker's contact

Fig. 6: Evaluation of the lateral wagon displacement. All the graphs present the superposition of results in the case of analytical and measured track with irregularities.

Figures 6-a,b refers to the case with no dampers, figures 6-c,d relates to the simulation with the non linear dampers. In all the cases the irregularities effect create a

low disturbance superimposed to the numerical solution with analytical track. Due to the motor eccentricity the lateral displacement of the wagon has a equilibrium position shifted, of about 0.015 m, from the starting position. In the more realistic damped case the wagon, after a quick transient, oscillates around that equilibrium position.

The comparison of linear and non linear contact model may be obtained by a first visual inspection of figures 6-a,c and figures 6-b,d. It is possible to observe that the two different solutions have the same results if we consider the mean value and the maximum amplitude.

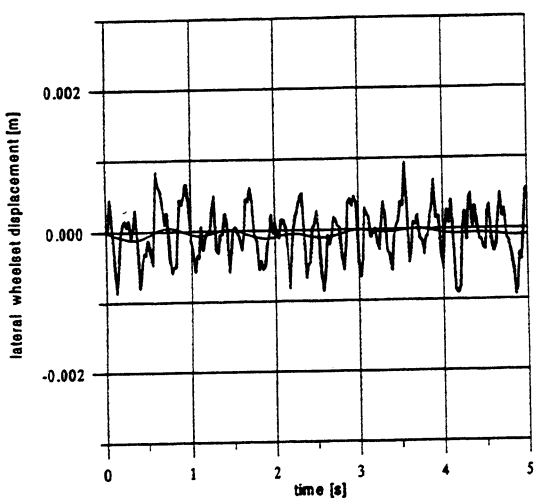

a) case with linear dampers and linearized Kalker's contact

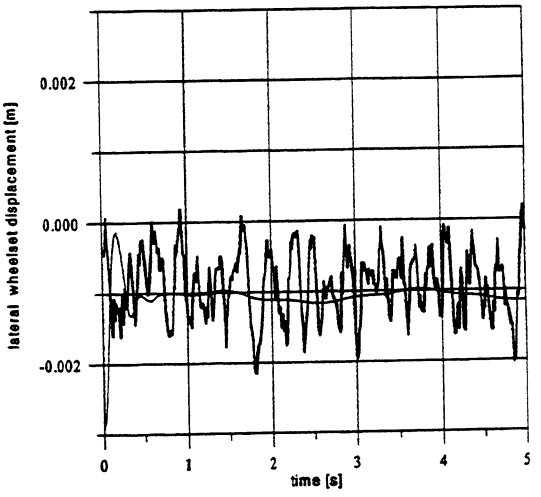

b) case with linear dampers and non linear Kalker's contact

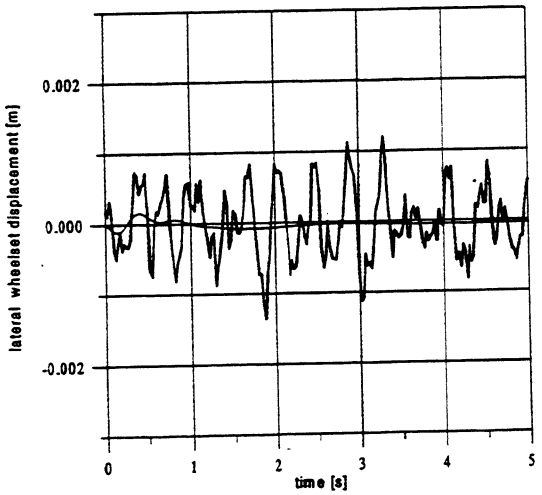

c) case with non linear dampers and linearized Kalker's contact

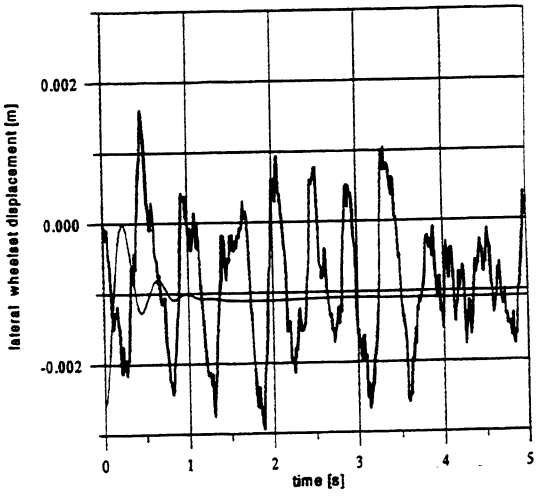

d) case with non linear dampers and non linear Kalker's contact

Fig. 7: Evaluation of the lateral wheelset displacement. All the graphs present the superposition of results in the case of analytical and measured track with irregularities.

Fig. 7-abcd show the *y* lateral displacement of the wheelset. The difference of linear and non-linear contact model is in these case more evident. In-fact in the case of the linearized Kalker contact theory (fig. 7a-c) the wheelset oscillates around the zero lateral displacement. In the case on non-linear theory (fig. 7b-d) the variation of the contact point allows the wheelset to oscillates around a shifted displacement.

CONCLUSIONS

The dynamic numerical simulation of a rail vehicle has been performed by using the ADAMS multibody computer code. Different transient simulation cases, taking into account the linear and non linear wheel-rail contact model, are compared.

Measured track data of an European benchmark has been introduced to evaluate the relative effect of the wheel-rail contact versus the track irregularities effect.

The results so obtained, even if as preliminary step of the research, allow to conclude that the linearized wheel-rail contact gives good results for critical speed analysis and wagon comfort studies also in presence of track irregularities.

The more realistic non-linear contact model allows to evaluate the wheelset and bogie behaviour but does not give any improvement to vehicle comfort analysis.

REFERENCES

[1] G. Diana, F. Cheli, S. Bruni, A. Collina: Modelli matematici per lo studio della interazione veicolo strutture - armamento. Ingegneria Ferroviaria, pp. 1066-1080 (1980).

[2] G. Diana, F. Cheli, S. Bruni, A. Collina: Dynamic Interaction between Rail Vehicles and Track High Speed Train. Vehicle System Dynamic, vol. 24, pp. 15-30 , (1995).

[3] C. Casini, G. Tacci: Studio di un modello matematico per la previsione della velocità critica di un veicolo ferroviario su un binario rettilineo senza difetti. Ing. Ferroviaria, pp. 262-275, (1978).

[4] J.J. Kalker: Review of Wheel Rail contact theories. Applied Mechanical Division Vol. 40, ASME PP. 77-92, (1980).

[5] J.J. Kalker: The computational of three dimensional contact with dry friction. International Journal of Numerical Methods in Engineering, Vol. 14, p. 1293-307 (1979).

[6] J.J. Kalker: Three-Dimensional Elastic Bodies in Rolling Contact. Kluwer Academic Publisher. 1990.

[7] ADAMS / SOLVER™. Reference Manual. Version 8.0. Mechanical Dynamics. 1994.

[8] ADAMS / RAIL 2281.User's Manual. Mechanical Dynamics GmbH ,Marburg. 1995.

[9] J.J. Kalker: *Book of Tables for the Hertzian Creep-Force Law*. Delft University internal report. 1996.

[10] B 176/3 Benchmark Problem Result and Assessment. European Rail Research Institute (ERRI) . Utrecht , August 1993

11th ADAMS European Users' Conference 1996
Frankfurt, November 19-20, 1996

Genetic Algorithms in Multi-link Front Suspension Optimisation

C.G.Franchi[1], F.Migone[2] and A.Toso[1]

Abstract

This paper addresses some aspects of race car suspension kinematics: analysis of non-conventional front suspensions, optimisation of suspension geometry and application of a non-conventional optimisation method.

The research aims to optimise vertical and steering kinematics properties of a race car front suspension by using a multi-link geometry, as the result of disconnecting the upper and lower triangles in the typical double wishbone pattern. The optimisation is carried out by means of a Genetic Algorithm (GA). Since GAs are task-independent, the user must provide only an evaluation function which returns some values when given a point in the search space. The points in the search space are the co-ordinates of the markers at the spherical joints between the suspension arms and the upright, while the evaluation functions are given by two user defined request functions. Two ADAMS models for vertical and steering suspension kinematics were developed. The optimisation procedure and the externally driven multi-body simulation run under the control of a FORTRAN code.

Finally, some examples of application and a brief discussion on the results are presented.

Introduction

Multi-link suspensions are broadly used in saloon-cars, both on front and rear axis, to achieve improvements in handling, stability and comfort. On the front axis, their enhanced dynamic geometry allows suitable toe, camber and scuff changes to improve alignment stiffness while maintaining a sufficient longitudinal compliance and comfortable ride. The independent kingpin mechanism allows desired changes in tire forces trial so as to obtain a greater steering control and stability (Ref. 1). On the rear axis, multi-link suspensions allow toe-in control so to ensure and promote stability when decelerating in cornering and to suppress deflections in the path of car in forward movement due to road unevenness. The enhanced dynamic geometry allows suitable camber changes, with respect to the body, to maintain optimal camber, with respect to the ground surface, in cornering and to suppress jacking effect (Ref. 2, 3). In general, with a multi-link suspension, the degrees of freedom increase and, by following the principle of one component per function, to best fit a greater number of design requirements is allowed.

Some of these requirements can be issued also for the race cars. The toe and scuff control leads to reduce the tires wear, while the independent caster and kingpin angles allow to control the tire forces trials and thus the steering torque. It has to be noted that the steering torque is perceived as one of many grip indicators and, particularly, as a sensor of ultimate car limit. Thus, by using a multi-link front suspension it seems possible to modify the driver's perception.

The optimisation of a multi-link suspension is not a trivial task because its kinematic parameters non linearly depend upon the whole suspension geometry. When more parameters have to be optimised, the existence of a unique optimal solution cannot be guaranteed and the use of a conventional optimisation method could lead to reach one of several local optimal solutions. Many features of the stochastic method known as Genetic Algorithm (GA) (Ref. 4, 5) suggest its use in solving this problem:

---

[1] Dallara Automobili Srl, v.Provinciale, 33 - 43040 Varano de' Melegari - PR
[2] Università degli Studi di Pisa

1. GA allows the treatment of all degrees of freedom as a single optimisation variable, instead of assigning a variable to anyone;
2. GA evaluates at any iteration a number of different solutions equal to the number of individual in the population. This fact guarantees that the solution will converge to a sufficient general optimum, regardless of the starting guess;
3. GA needs only to evaluate the objective functions, without any information on their gradients;
4. GA shows all of the generality of simulated annealing and other stochastic methods, but its strength comes from the use, besides random searching technique, of an evolutionary criterion in selection. It guarantees equilibrium in selecting good solutions among the available ones and in exploiting new directions in the solution space.

Race Car Front Suspension

On modern open wheels race cars, the standard suspension has a double wishbone geometry and the unique layout variation stay in using a push or pull rod. The addition of further elements is discouraged by the need to minimise the suspension weight and component number, while that of further joints increases suspension compliance and backlashes. On race car the minimisation of this parameters is the main concern because of the poor attention to comfort and of small value of tire lateral slip that force to reduce undesired suspension movements.

On the other hand, the area between chassis and wheel has to be kept clean to guarantee a good air flow to the car lateral side. Hence, the suspension elements have, as far as possible, to be kept out the area between chassis and wheel and have a reduced frontal section. Thus they appear as in Figure1, as beams with a high aspect ratio.

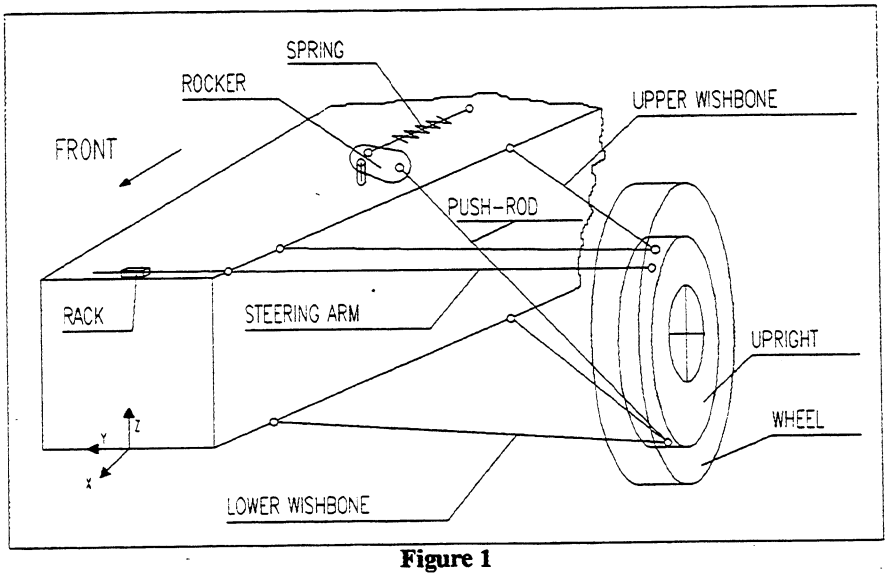

Figure 1

The kinematic analysis of this front suspension is carried out by considering two motions:

Vertical: a vertical motion is superimposed to the wheel with respect to the chassis, while holding the rack. In this way, the bump behaviour of the suspension can be analysed without any steering effect.

Steering: a motion is superimposed to the rack with respect to the chassis. The steering behaviour of the suspension can so be analysed. It is also useful to evaluate the toe changes when the wheel is all inside or outside steered. Thus, a vertical kinematic analysis is required in the extreme steering positions.

Since the above cited constraints on the race car suspension, the only possibility to achieve a multi-link geometry without adding suspension elements seems that to open the upper, the lower or both the triangles of the double wishbone. In this way we add till six degrees of freedom to our suspension. In this work we considered this model of suspension, or some of its simplified version, to develop the optimisation method; the optimisation variables being the co-ordinates of points 6, 7, 19 and 20, free to float on the upright. The space required for parts and joints mounting represents a constraint in points floating.

The ADAMS Model of Multi-link Front Suspension

The multi-link suspension has been modelled as a rigid multi-body system by means of ADAMS (Ref.6). Figure 2 presents the parts and the joints forming the model. The analysis of vertical kinematics has been carried out by superimposing a motion to the translation joint 22 from -10 to 40 mm, while locking the translation joint 21. The analysis of steering kinematics has been carried out by superimposing a motion to the

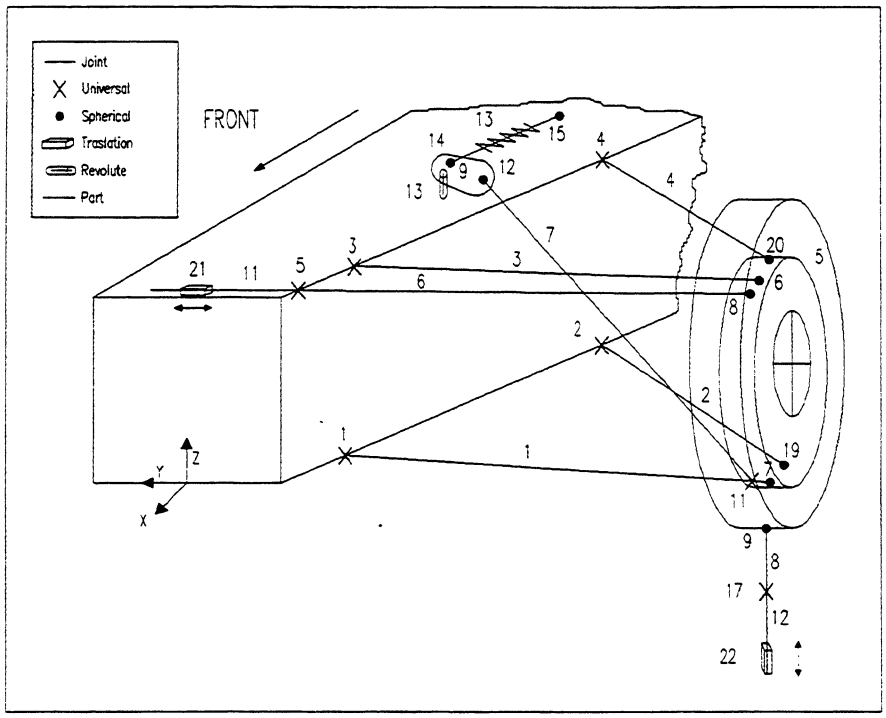

Figure 2

translation joint 21 from -15 to 15 mm, while locking the translation joint 22.

The suspension motions are assigned by a user defined motion subroutine (MOTSUB) (Ref.7), while vertical and steering kinematic parameters are evaluated in accordance with SAE definitions (Ref.8) by means of two user defined request subroutines (REQSUB) (Ref.7). In this sense, we have to note that, as the non conventional suspension, the kingpin and roll axis cannot be evaluated by simple geometrical constructions. In accordance to Euler-Chasles' theorem, they are evaluated as instantaneous rotation axis of some rigid bodies.

Genetic Algorithm

A GA is a random optimisation method in which some operators guide the search toward a favourable region in the solution space by mimicking natural selection. GA does not work over a single point in the solution space, but over a set of N_I elements and operates on their codification by means of probabilistic and evolutionary criteria. Any point in the solution space is called *individual*; the set of N_I individuals is called *population*.

Each one of the n co-ordinates of i^{th} individual in the solution space is binary coded by means of a fixed length sub-string (Ref.9). The length of the sub-string depends upon the type of co-ordinate to be coded and upon its value. As a matter of fact, a Boolean co-ordinate can be coded by using a single bit, while the codification of integer or real co-ordinates depends upon their range and resolution. It must be emphasised that the co-ordinates of the solution space can also be non homogeneous and that their codification rules can be wholly different.

The n sub-strings thus obtained are joined to form the ith individual's genetic code; any coded individual is called *chromosome*. In Figure 3 is presented a simple example of a possible binary coding.

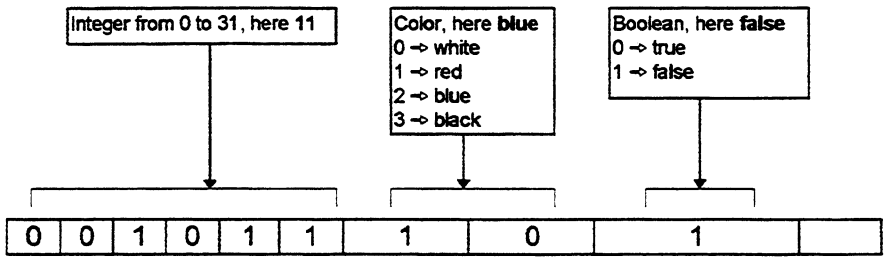

Figure 3

For any individual the objective functions can be analysed and some fitness indices evaluated. GA tests the population's strings by analysing the performance indices. In this sense, two approaches can be followed:

Single functional optimisation - A single performance index, here called p_i, is evaluated for i^{th} individual as related to a single objective function. It is scaled to produce the fitness value f_i by:

$$f_i = p_i / \sum p_i \qquad (1)$$

The fitness value of each i^{th} individual determines its probability of survival through the evolutionary process; i.e.: the probability to be selected as parent for chromosomes recombination.

Multifunctional optimisation - M performance indices, here called p_i^j, with j=1,M, are evaluated for i^{th} individual as related to as many as objective functions. They are analysed to give a single fitness value f_i by means of a variant of the Pareto's algorithm well discussed in Ref. 5. Among the M indices, M_1 are selected as primary and M_2 as secondary; where the following condition holds:

$$M = M_1 + M_2 \qquad (2)$$

The individuals are ranked under a dominance criterion on the M_1 primary indices. The individuals are further ranked under a dominance criterion on the M_2 secondary indices. At the end of this two steps ranking procedure, the individual's rank, scaled to unit sum, represents its fitness value.

Once the fitness values have been evaluated for all the individuals, the evolutionary procedure can begin. It works by applying three classical operators in genetic evolution: reproduction, crossover and mutation, presented in Ref. 5, 10, 11. By repeating the genetic selection, it gives arise to N_G generation and the final one is accepted as optimal.

The Programming Code

The optimisation process consists in an iterative procedure managed by a FORTRAN program *algen*. It program provides both the individuals' selection through the GA (Ref.12) and their evaluation through ADAMS simulations. The interface between *algen* code and the ADAMS environment is provided by the FORTRAN code *driver_adams* that uses the ADAMS callable functions (Ref.7). The structure of the program *algen* can be represented by:

1. Random generation ➲ First generation;
2. Loop on whole the generations;
   3. Convert the *chromosomes* ➲ values of the optimisation variables;
   4. Run *driver_adams* ➲ objective functions:
      A. Steering kinematics analysis:
         a. loading of the ADAMS model for steering kinematics;
         b. loop on whole the individuals of the population;
            c. modify the markers' location;
            d. carry out the simulation;
      B. Vertical kinematics analysis:
         a. loading of the ADAMS model for vertical kinematics;
         b. loop on whole the individuals of the population;
            c. modify the markers' location;
            d. carry out the simulation;
   4. Analyse objective functions ➲ fitness values;
   5. Run the genetic operators ➲ next population;

Numerical Examples

To test the proposed method, some examples have been analysed. We tested a population of 200 individuals over 60 generations, while the crossover and the mutation rates are fixed at .6 and .001 respectively (Ref. 5). We defined the desired vertical and steering kinematic behaviour of the suspension as in Figures 4 and 5. It has to be noted that the desired behaviours for different parameters could be on conflict among them. Thus, the optimisation process can only reach an optimal trade-off between tendencies on conflict.

In Example 1 we considered only the toe evolution in vertical kinematics as objective function by forcing its value to move as less as away from zero. Figure 6 proves that the target has been reached.

In Example 2 both the toe and wheelbase change in vertical kinematics are objective functions. We forced their values to move as less as away from zero by applying a Pareto's algorithm. Figure 7 presents the results.

In Example 3 we forced caster trail to be as close as possible to the desired path in steering kinematics and toe evolution in vertical kinematics to move as less as away from zero. We used a modified Pareto's algorithm with first ranking on the caster offset and the second one on toe. The results, presented in Figure 8, prove the effectiveness of the optimisation procedure.

Finally, in Example 4 we considered a complex optimisation on nine parameters by means of a modified Pareto's algorithm. In the first step we ranked the individuals on: camber and kingpin offset paths in steering kinematics, toe and bump-steer in vertical kinematics. In the second one, we did on caster trail and steering ratio paths in steering kinematics and camber path, wheelbase and track change in vertical kinematics. The results in Figures 9 prove that the target has been well reached.

Concluding Remarks

In this paper we proposed the GA as optimisation method to face the kinematic analysis of non-conventional front suspensions. We developed a general algorithm that integrates ADAMS and GA, via ADAMS callable functions. The first is used as slave to generate the values of the objective functions, while the second uses those to carry out the optimisation. The results, although obtained for simple examples and without exploiting all the available degrees of freedom, confirm all of the promises and the method seems suitable for more general applications.

However, the research remain open and many aspects of the herein presented method have to be investigated before it could become an effective engineering tool in race car design. In particular, the optimisation strategy has to be refined to define the proper ranking order in modified Pareto's algorithm, while the programming code itself has to be optimised to considerably reduce the analysis time.

References

[1] Murakami T., Uno T., Iwasaki H. and Noguchi H., *Development of a New Multi-Link Front Suspension*, SAE Paper No. 890179, 1989.

[2] Tsukuda Y., Tsubota Y., Tonomura H., Noguchi H., *Development of a New Multi-Link Rear Suspension*, SAE Paper No. 881774, 1988.

[3] Andersson J.E., Bane O. and Larsson A., *Volvo 760 GLE Multi-Link Rear Axle Suspension*, SAE Paper No. 890082, 1989.

[4] Holland J.H., *Adaptation in natural and artificial systems*, University of Michigan Press, Ann Arbor, 1975.

[5] Goldberg D.E., *Genetic Algorithms in Search, Optimisation and Machine Learning*, Addison-Wesley, Reading, MA, 1989.

[6] ADAMS/SOLVER Reference Manual - version 8.0, *Mechanical Dynamics*, 2301 Commonwealth Blvd., Ann Arbor - MI, Nov.15, 1994.

[7] ADAMS/SOLVER Subroutines Reference Manual - version 8.0, *Mechanical Dynamics*, 2301 Commonwealth Blvd., Ann Arbor - MI, Nov.15, 1994.

[8] *Vehicle Dynamics Terminology*, SAE J740e, Society of Automotive Engineers, Warrendale, PA, USA.

[9] Caruana R.A., Schaffer J.D., *Representation and hidden bias: gray vs. binary coding for genetic algorithms*, In Proceeding of Fifth International Conference on Machine Learning, 1988, pp.153-161.

[10] Davis L., *Handbook of Genetic Algorithms*, Van Nostrand Reinhold, NY, USA, 1991.

[11] De Jong K., *Adaptive System Design: A Genetic Approach*, IEEE Transaction on System Science and Cybernetics, vol.SMC-10, n.9, 1980, pp.566-574.

[12] Franchi C.G. and Gallieni D., *Genetic-Algorithm-Based Procedure for Pretest Analysis*, AIAA Journal, vol.33, n.7, July 1995, pp.1362-1364.

KINEMATICS

4 Nov 1996 17:31

Data File : Reference

Suspension : Optimal Parameters

m.ruo/m.mol statico	.8986
c.rollio statico [mm]	-5.1533
Dcamber/Dz [gr/mm]	-.0114
Dcamber/Drollio [gr/gr]	.8639
Dtoe-out/Dz [gr/mm]	.0023
DHcr / Dz [mm/mm]	-.0810
Dcarr/Dz [mm/mm]	-.0056
Dpasso/Dz [mm/mm]	.0603
Drapp/Dz [--/mm]	-.0058

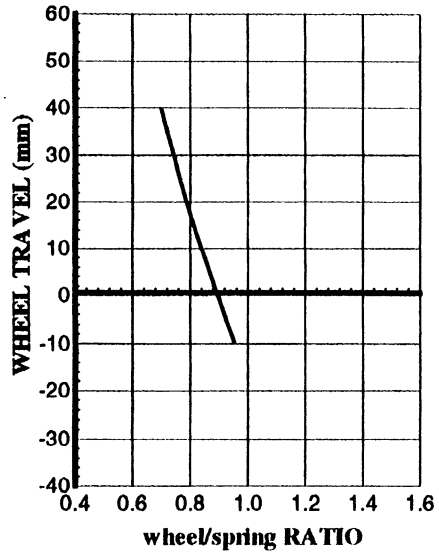

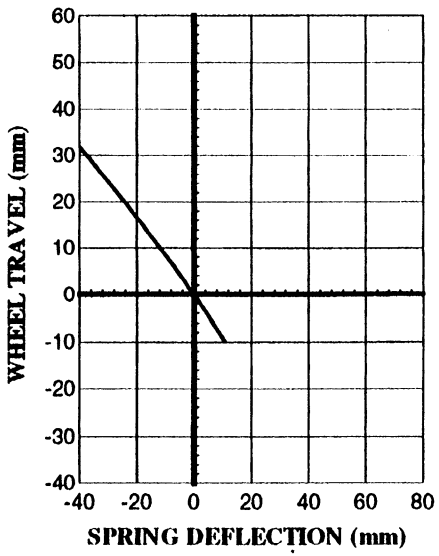

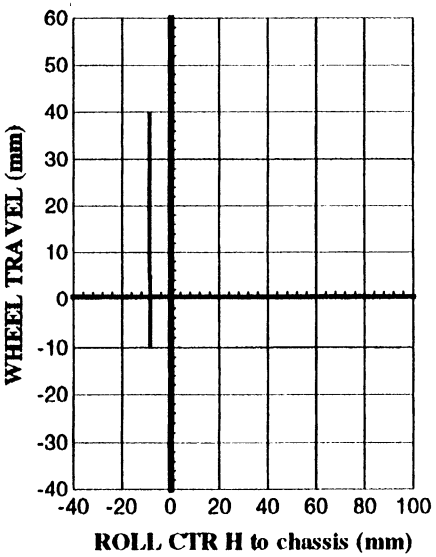

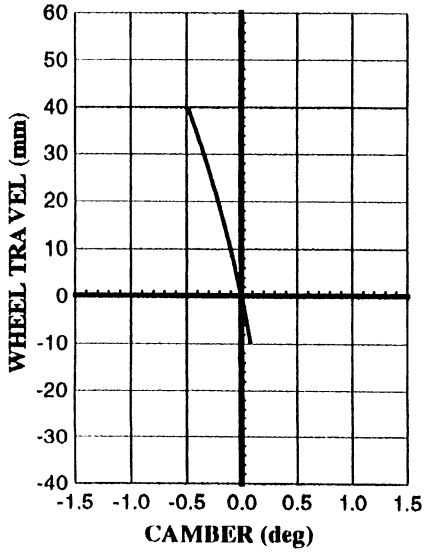

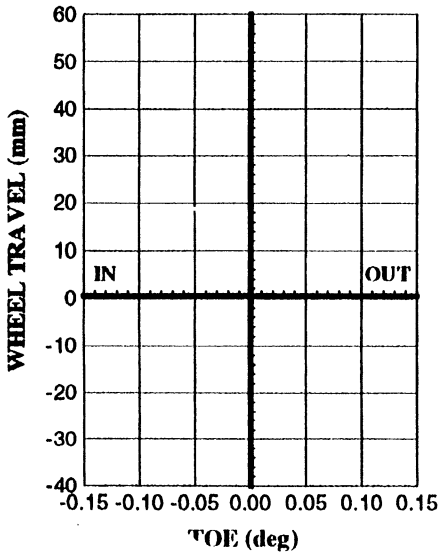

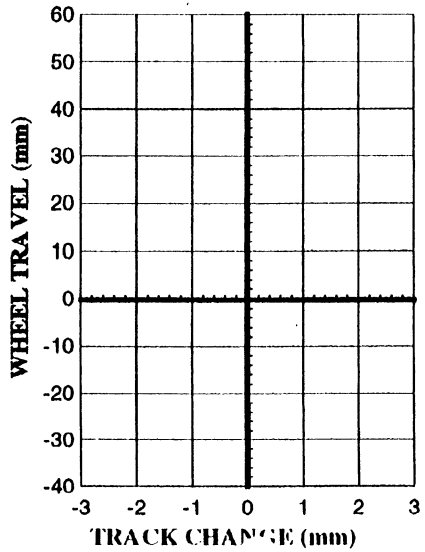

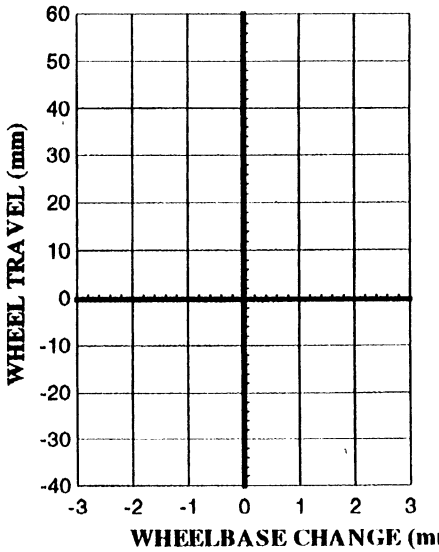

Figure 4

STEER KINEM.

4 Nov 1996 17:40

Data File : Reference

Suspension : Optimal Parameters

r.sterzo statico	13.6100
diam. pignone [mm]	15.0990
caster [gr]	9.0742
kingpin [gr]	9.8521
BT-long [mm]	21.3353
BT-lat [mm]	49.0818
m.crem. [mm]	15.0000
A.RUOTA EXT [gr]	8.0238
A.RUOTA INT [gr]	-8.7654
Dcamber/Druo[gr/gr]	-.1597
Dscuot /Druo[mm/gr]	.2015
Drapp /Druo[/gr]	.1442
Dpasso /Druo[mm/gr]	.8566
Dcam. /Druo[mm/gr]	.3724
D BTlon/Druo[mm/gr]	.6072
D BTlat/Druo[mm/gr]	-.1803
Dcaster/Druo[gr/gr]	.2189
Dkingp /Druo[gr/gr]	.0647

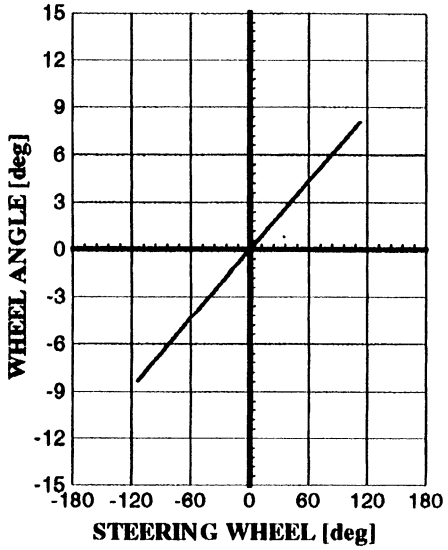

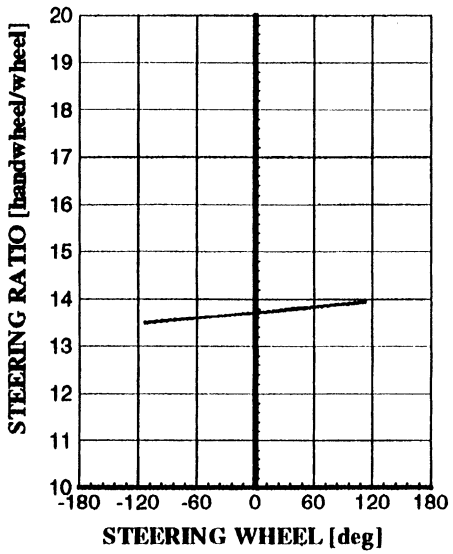

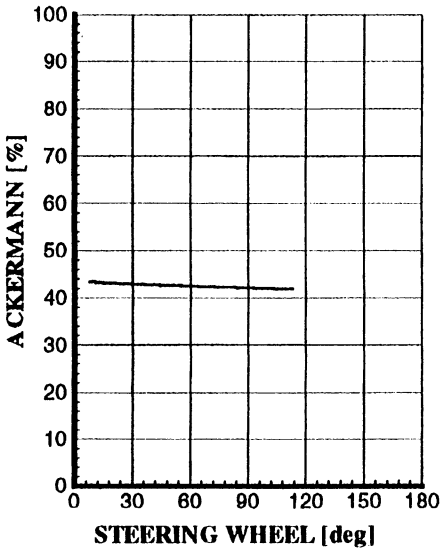

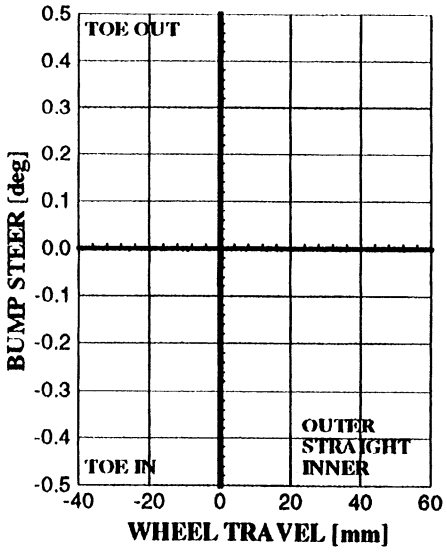

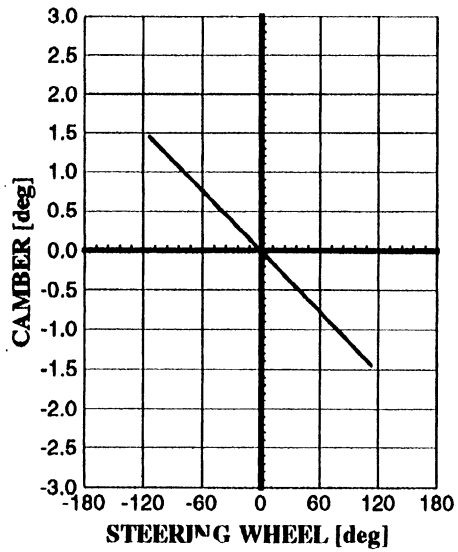

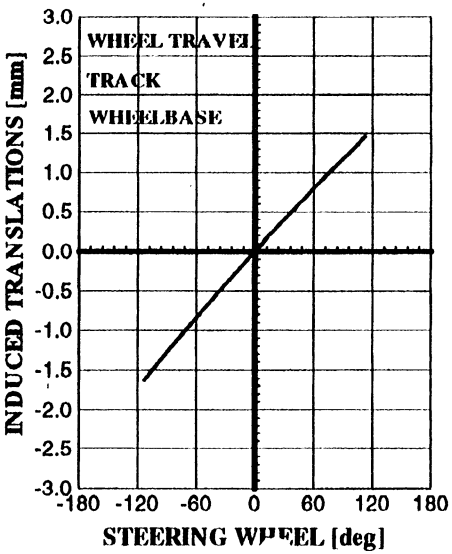

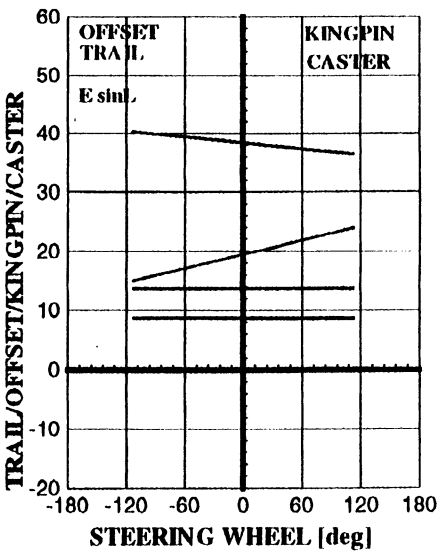

Figure 5

KINEMATICS

4 Nov 1996 17:31

Data File : Example 1

Suspension : Objective function: Toe

m.ruo/m.mol statico	.9025
c.rollio statico [mm]	-2.5434
Dcamber/Dz [gr/mm]	-.0128
Dcamber/Drollio [gr/gr]	.8466
Dtoe-out/Dz [gr/mm]	-.0001
DHcr / Dz [mm/mm]	-.0795
Dcarr/Dz [mm/mm]	-.0021
Dpasso/Dz [mm/mm]	.0825
Drapp/Dz [--/mm]	-.0058

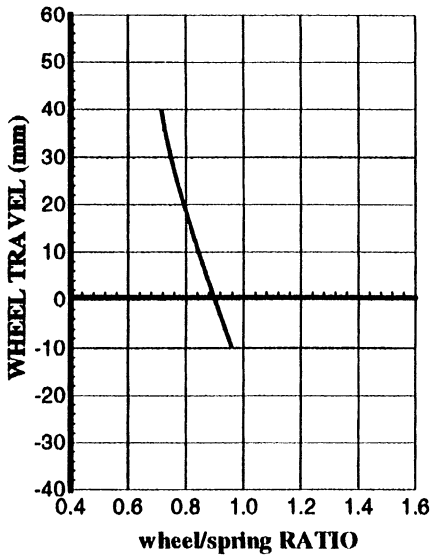

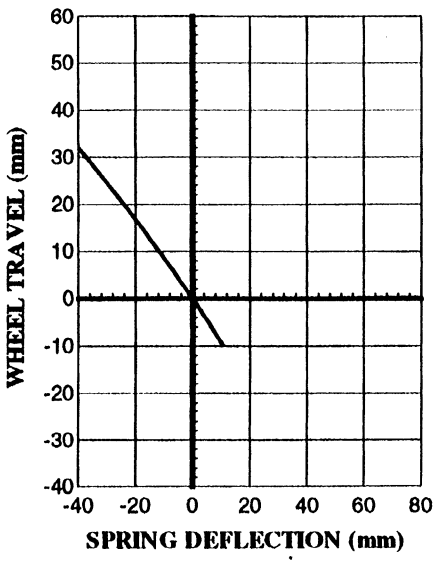

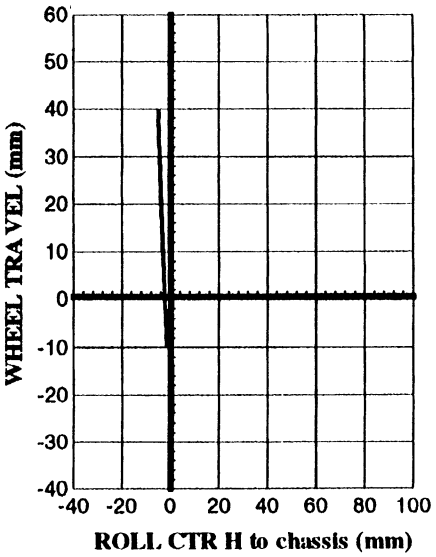

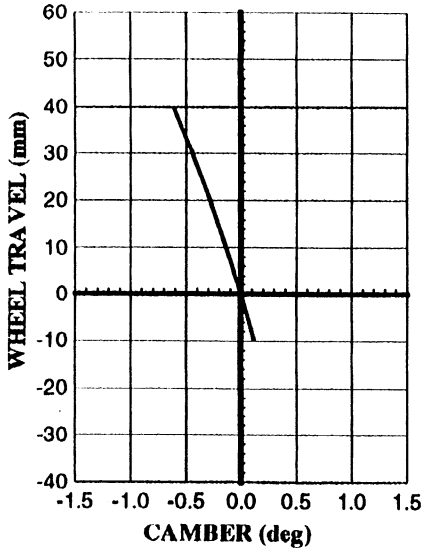

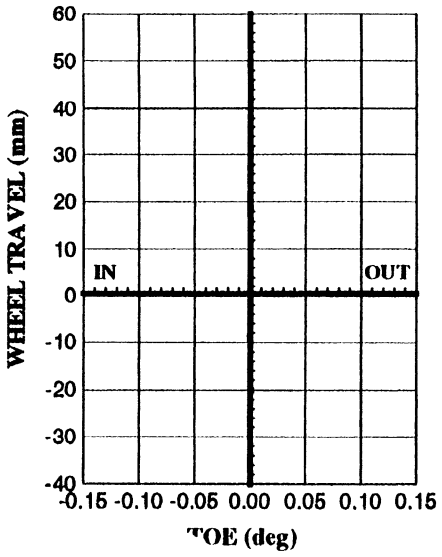

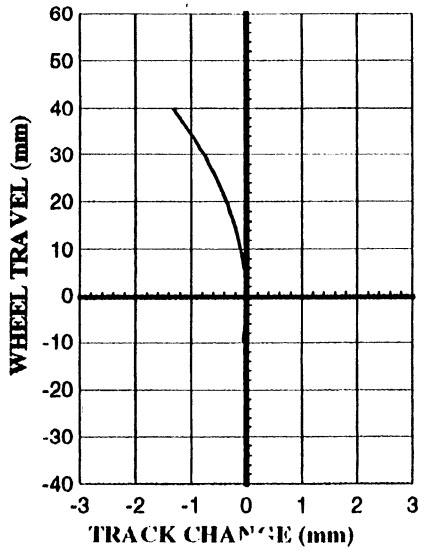

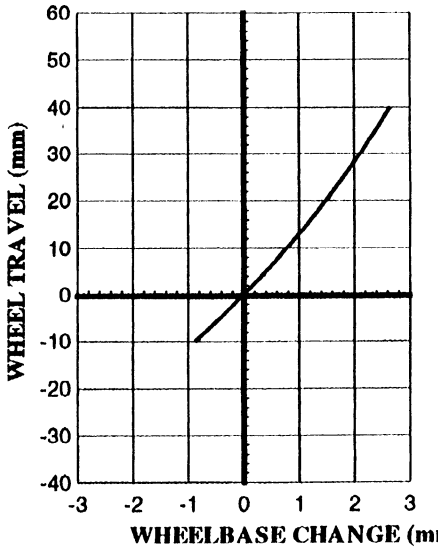

Figure 6

STEER KINEM.

4 Nov 1996 17:40

Data File : Example 1

Suspension : Objective function: Toe

Figure 6b

r.sterzo statico	12.3729
diam. pignone [mm]	15.0990
caster [gr]	7.8262
kingpin [gr]	3.2530
BT-long [mm]	17.8846
BT-lat [mm]	67.1904
m.crem. [mm]	15.0000
A.RUOTA EXT [gr]	9.0708
A.RUOTA INT [gr]	-9.3902
Dcamber/Druo[gr/gr]	-.1375
Dscuot /Druo[mm/gr]	.1789
Drapp /Druo[/gr]	.0475
Dpasso /Druo[mm/gr]	1.1727
Dcarr. /Druo[mm/gr]	.3121
D BTlon/Druo[mm/gr]	.4307
D BTlat/Druo[mm/gr]	.1457
Dcaster/Druo[gr/gr]	.1562
Dkingp /Druo[gr/gr]	-.0537

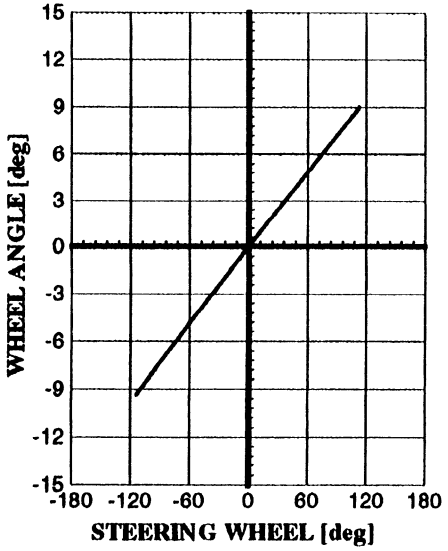

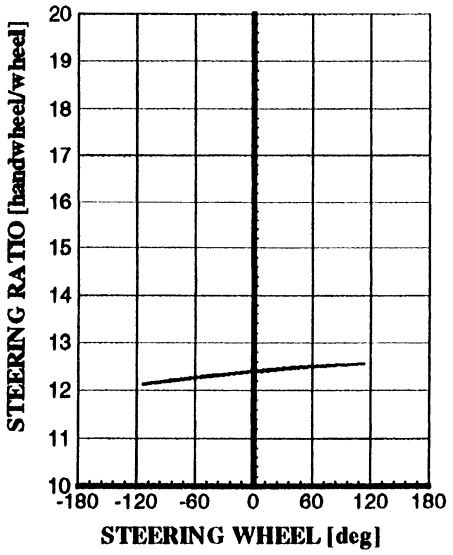

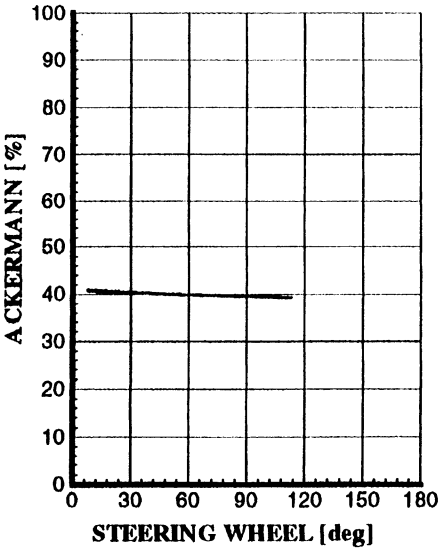

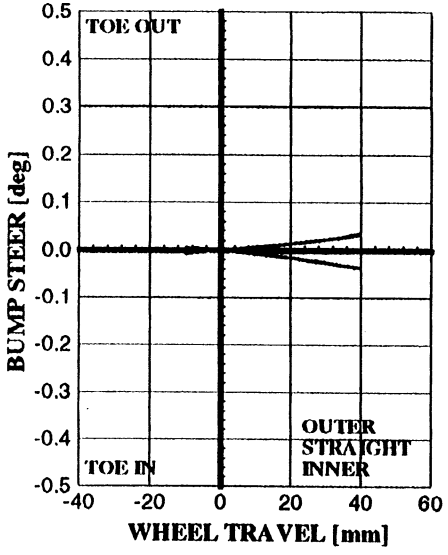

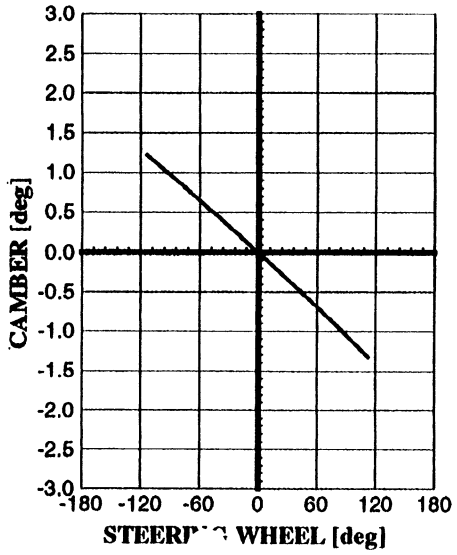

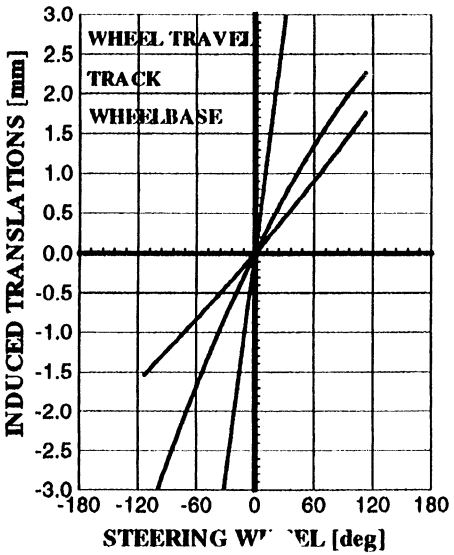

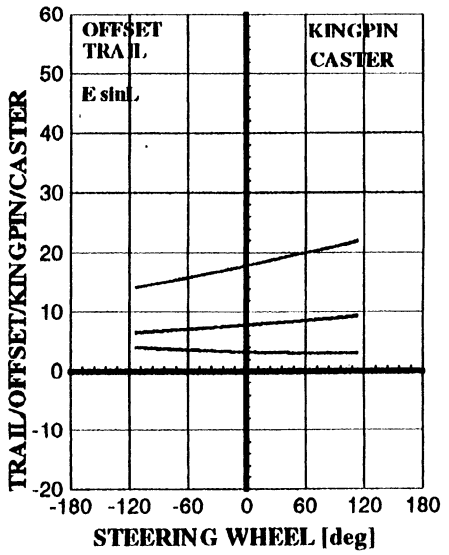

KINEMATICS

4 Nov 1996 17:40

Data File : Example 2

Suspension : Objective functions: Toe, Wheelbase Change

Figure 7

m.ruo/m.mol statico	.9011
c.rollio statico [mm]	-4.3783
Dcamber/Dz [gr/mm]	-.0119
Dcamber/Drollio [gr/gr]	.8583
Dtoe-out/Dz [gr/mm]	-.0001
DHcr / Dz [mm/mm]	-.0915
Dcarr/Dz [mm/mm]	-.0048
Dpasso/Dz [mm/mm]	.0681
Drapp/Dz [--/mm]	-.0059

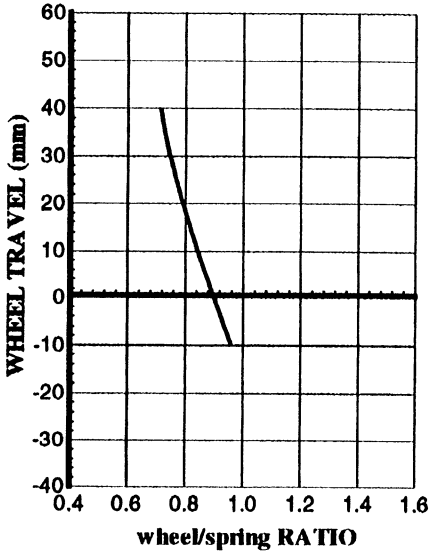

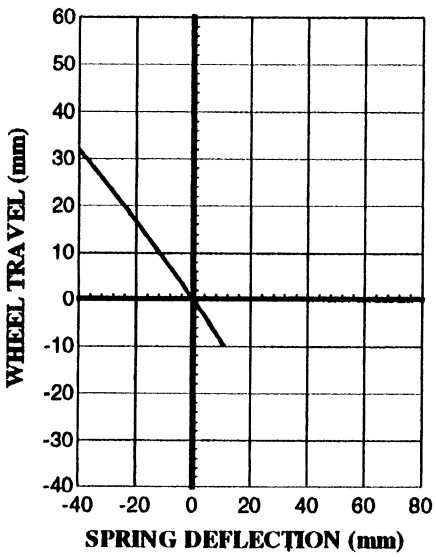

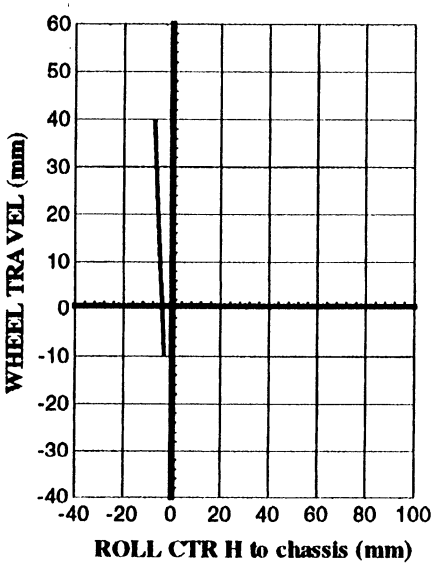

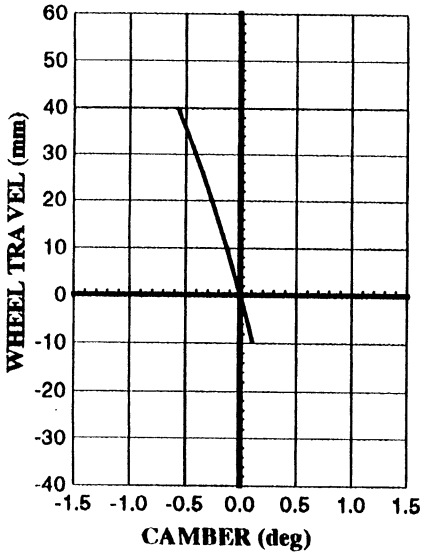

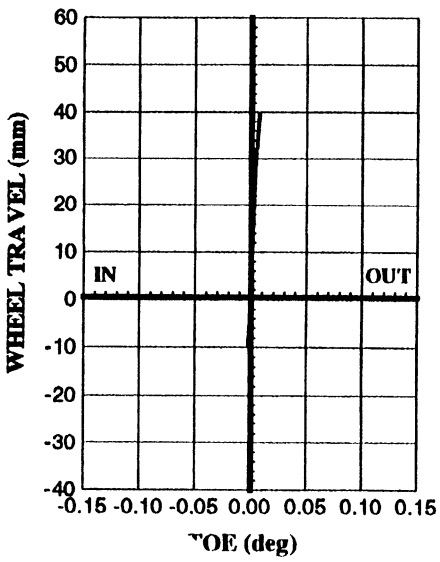

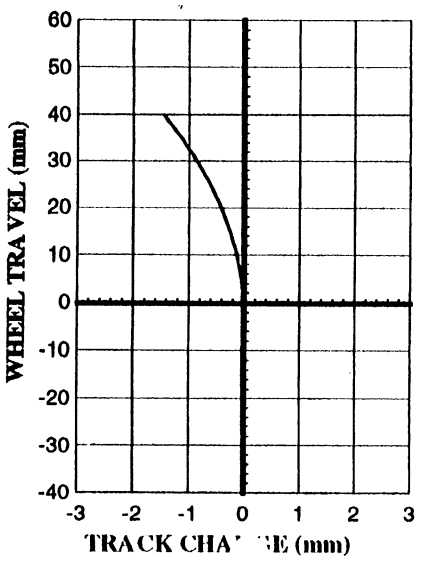

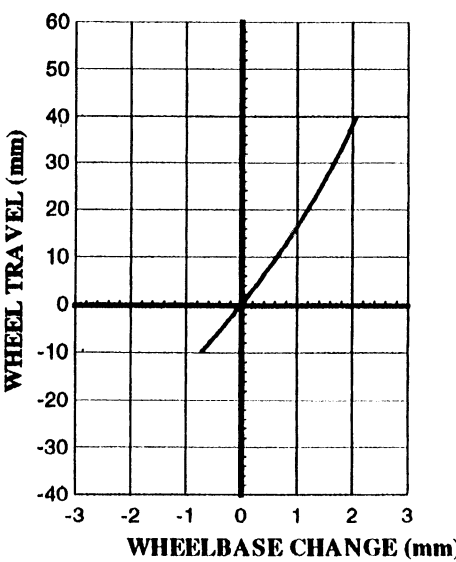

STEER KINEM.

4 Nov 1996 17:40

Data File : Example 2

Suspension : Objective functions: Toe, Wheelbase Change

Figure 7b

r.sterzo statico	10.6458
diam. pignone [mm]	15.0990
caster [gr]	5.6554
kingpin [gr]	3.5485
BT-long [mm]	11.9293
BT-lat [mm]	85.6118
m.crem. [mm]	15.0000
A.RUOTA EXT [gr]	10.5836
A.RUOTA INT [gr]	-10.9191
Dcamber/Druo[gr/gr]	-.0990
Dscuot /Druo[mm/gr]	.1351
Drapp /Druo[/gr]	.0322
Dpasso /Druo[mm/gr]	1.4942
Dcarr. /Druo[mm/gr]	.2082
D BTlon/Druo[mm/gr]	.6914
D BTlat/Druo[mm/gr]	.2607
Dcaster/Druo[gr/gr]	.2531
Dkingp /Druo[gr/gr]	.0960

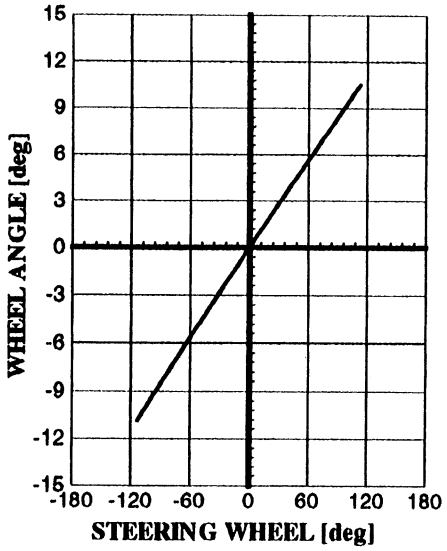

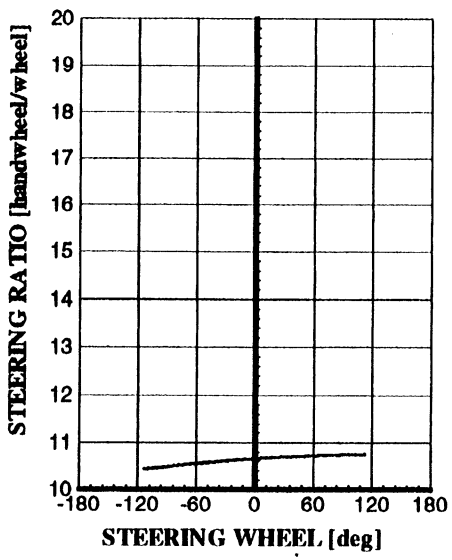

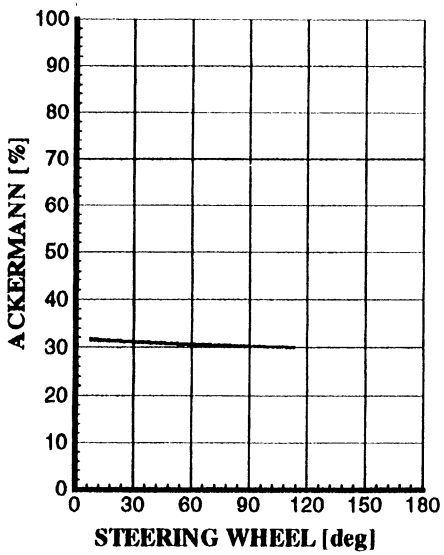

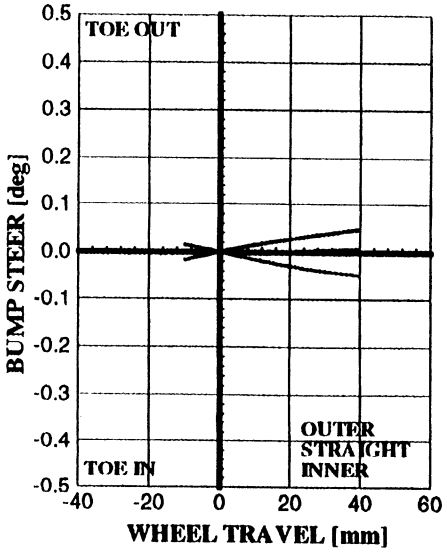

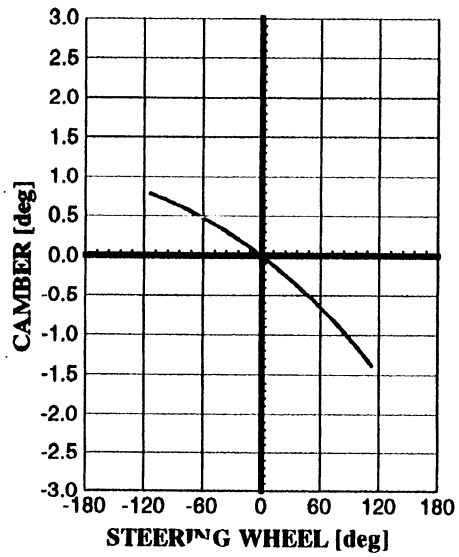

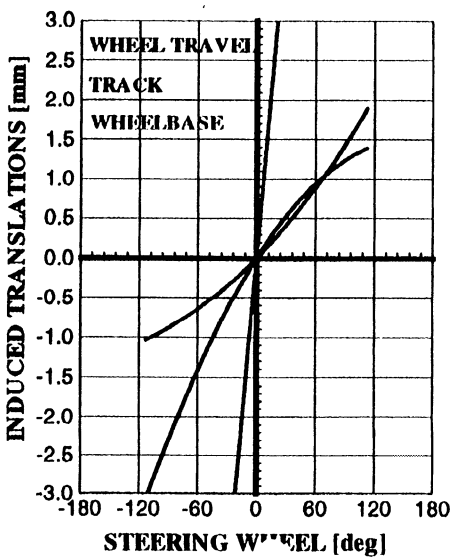

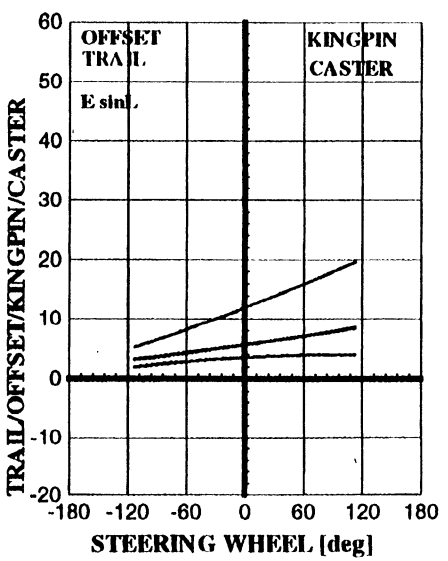

KINEMATICS

4 Nov 1996 17:31

Data File : Example 3

Suspension : Objective functions: 1st Trail, 2nd Toe

m.ruo/m.mol statico	.9022
c.rollio statico [mm]	-2.3013
Dcamber/Dz [gr/mm]	-.0126
Dcamber/Drollio [gr/gr]	.8488
Dtoe-out/Dz [gr/mm]	.0010
DHcr / Dz [mm/mm]	-.0698
Dcarr/Dz [mm/mm]	-.0027
Dpasso/Dz [mm/mm]	.0854
Drapp/Dz [--/mm]	-.0058

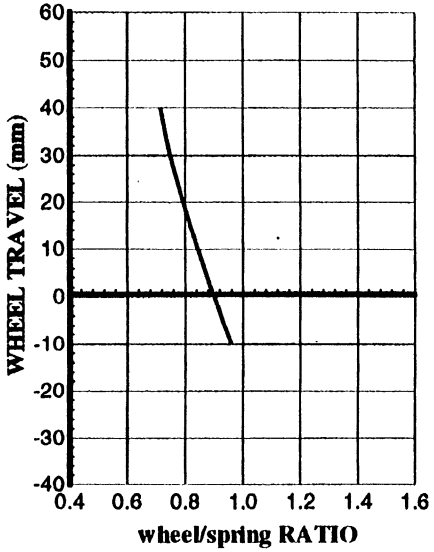

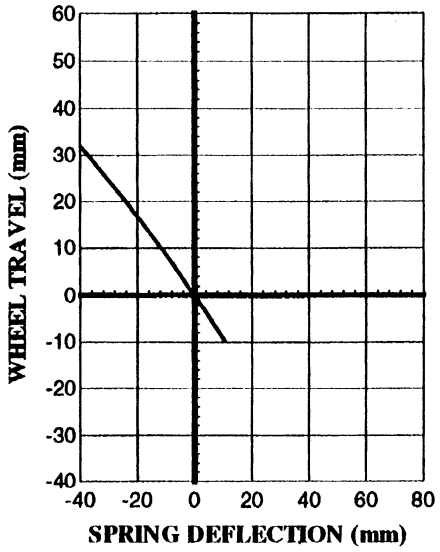

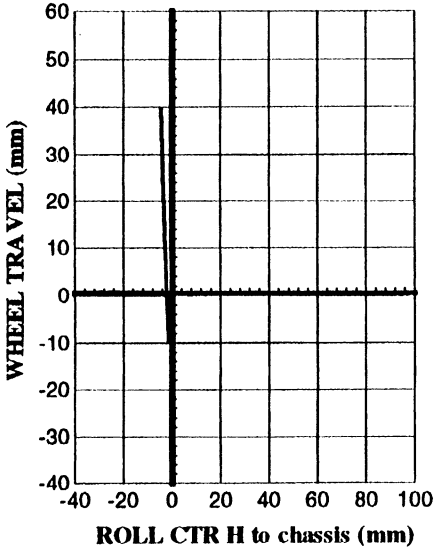

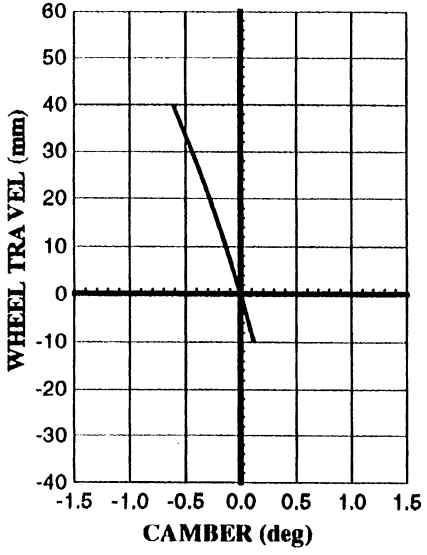

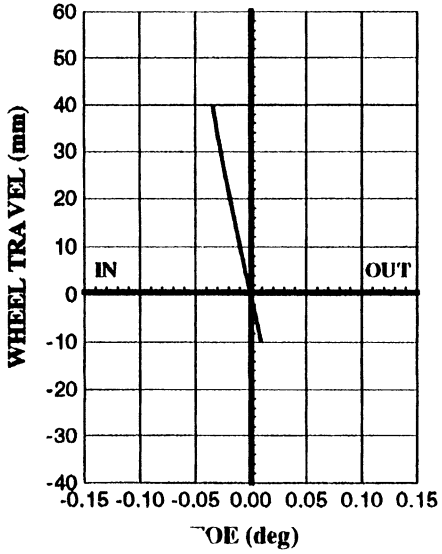

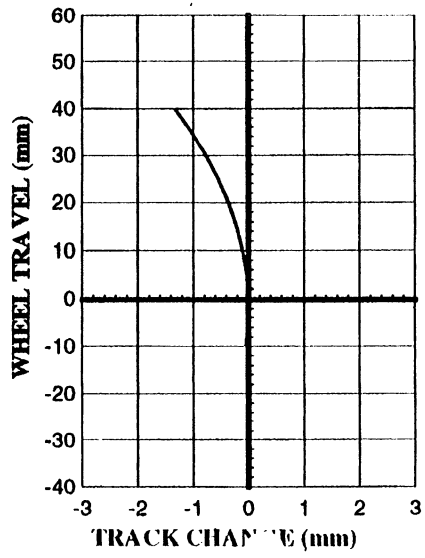

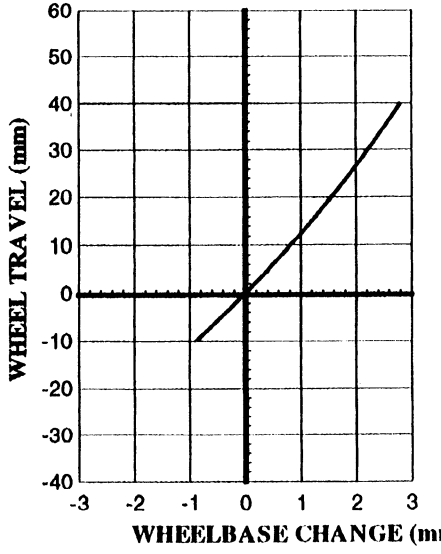

Figure 8

STEER KINEM.

4 Nov 1996 17:40

Data File : Example 3

Suspension : Objective functions: 1st Trail, 2nd Toe

r.sterzo statico	12.6974
diam. pignone [mm]	15.0990
caster [gr]	7.5682
kingpin [gr]	8.0082
BT-long [mm]	17.1739
BT-lat [mm]	54.1935
m.crem. [mm]	15.0000
A.RUOTA EXT [gr]	8.8231
A.RUOTA INT [gr]	-9.1529
Dcamber/Druo[gr/gr]	-.1329
Dscuot /Druo[mm/gr]	.1678
Drapp /Druo[/gr]	.0529
Dpasso /Druo[mm/gr]	.9458
Dcarr. /Druo[mm/gr]	.2997
D BTlon/Druo[mm/gr]	.3093
D BTlat/Druo[mm/gr]	.4858
Dcaster/Druo[gr/gr]	.1124
Dkingp /Druo[gr/gr]	-.1761

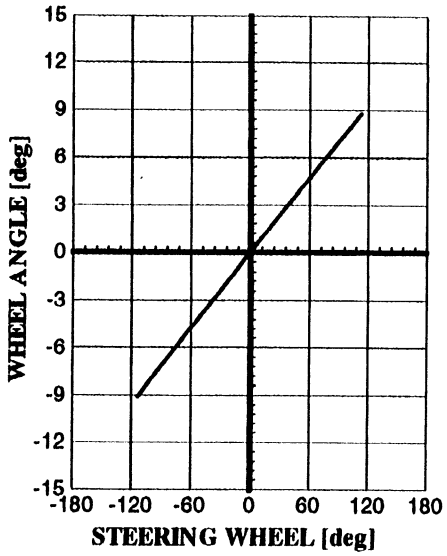

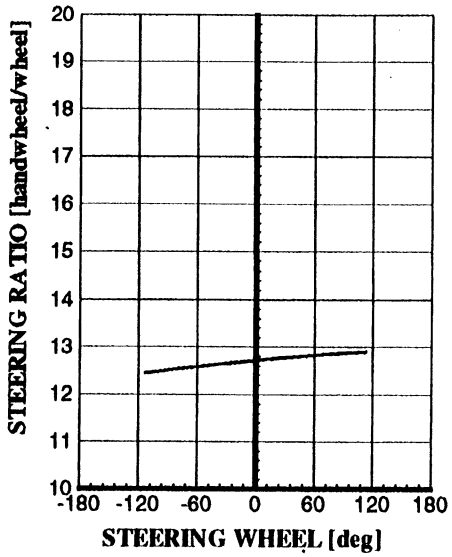

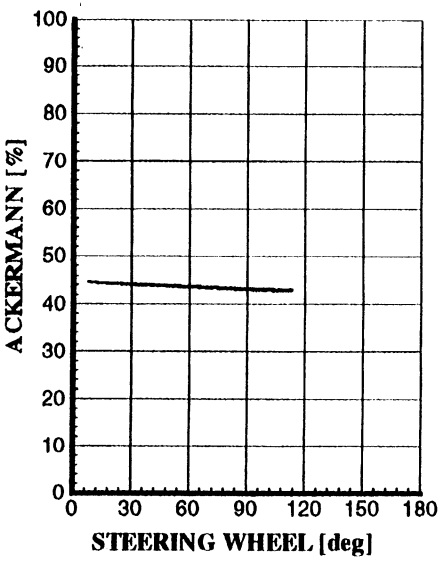

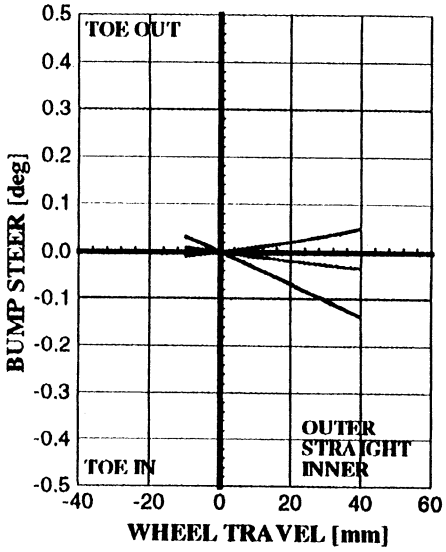

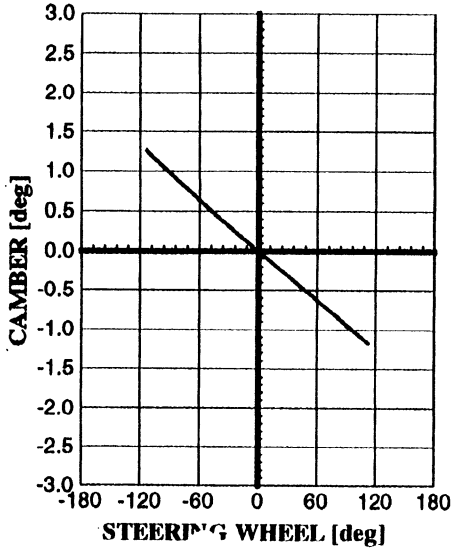

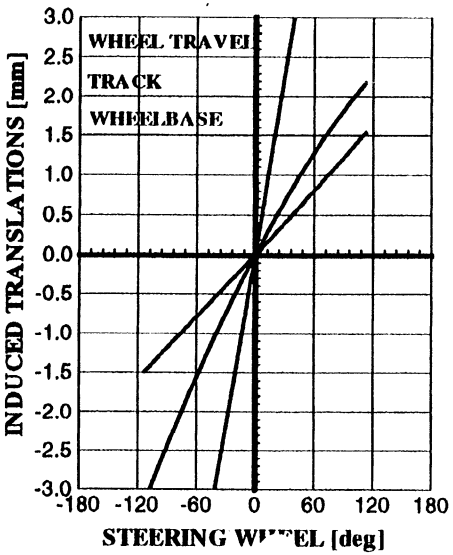

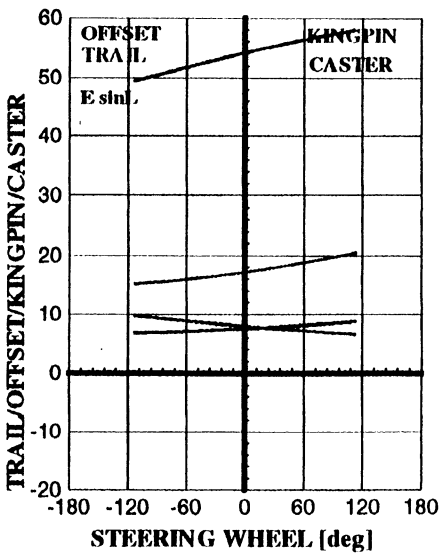

Figure 8b

KINEMATICS

4 Nov 1996 17:31

Data File : Example 4

Suspension : Objective functions: 1st Vertical Camber, Toe, Offset, Bump Steer
2nd Steering Camber, Trail, Wheelbase, Track, Steering Ratio

m.rio/m.mol statico	.8995
c.rollio statico [mm]	-5.5557
Dcamber/Dz [gr/mm]	-.0108
Dcamber/Drollio [gr/gr]	.8712
Dtoe-out/Dz [gr/mm]	.0013
DHcr / Dz [mm/mm]	-.1008
Dcarr/Dz [mm/mm]	-.0079
Dpasso/Dz [mm/mm]	.0607
Drapp/Dz [--/mm]	-.0058

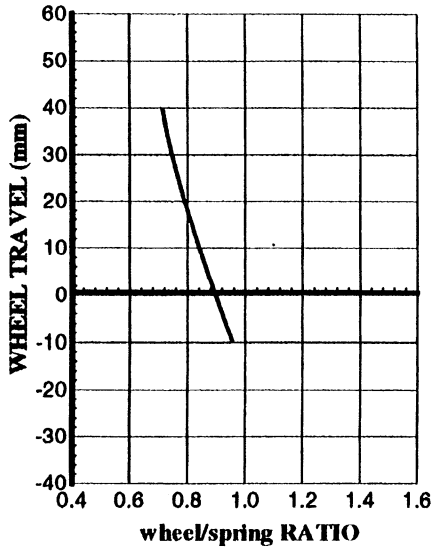

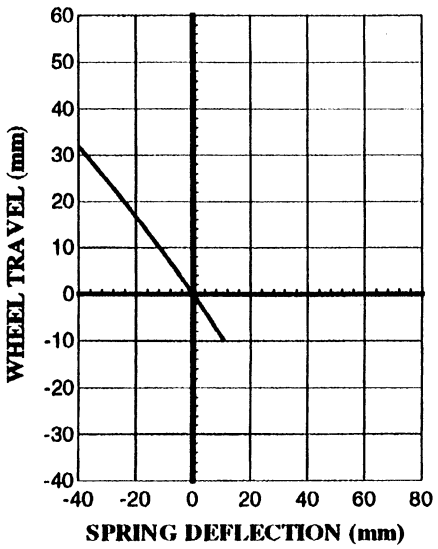

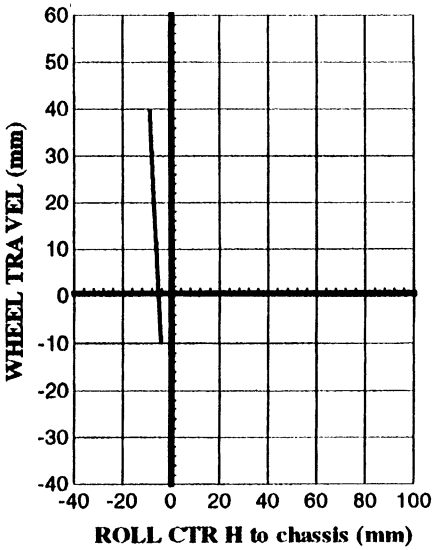

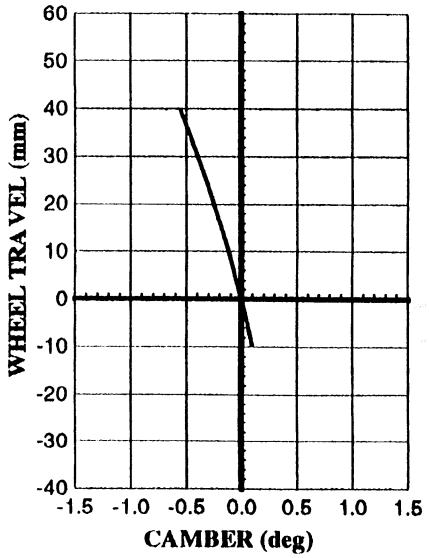

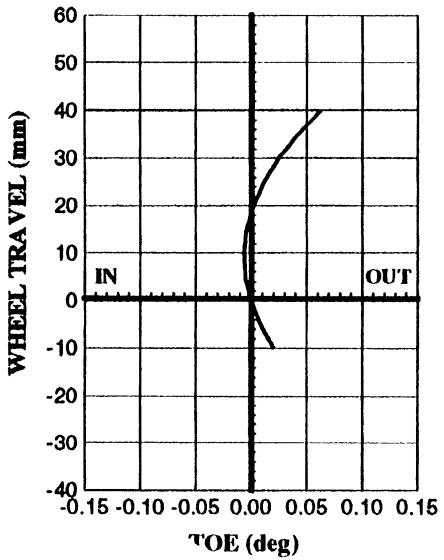

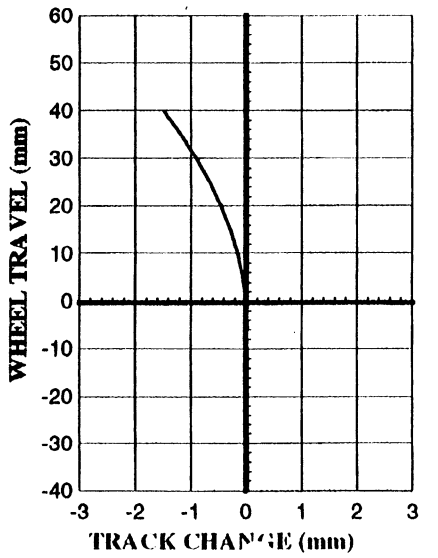

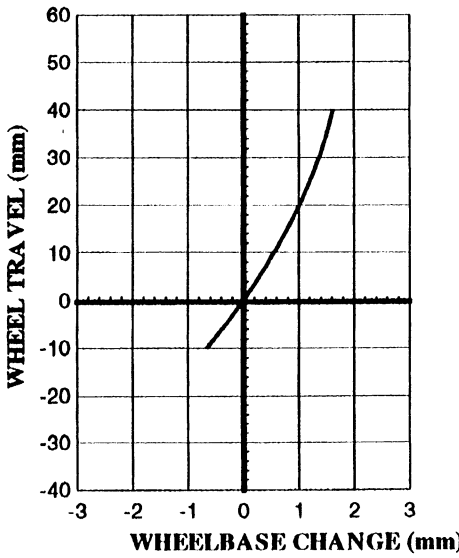

Figure 9

STEER KINEM.

4 Nov 1996 17:40

Data File : Example 4

Suspension : Objective functions: 1st Vertical Camber, Toe, Offset, Bump Steer
2nd Steeering Camber, Trail, Wheelbase, Track, Steering Ratio

r.sterzo statico	13.6100
diam. pignone [mm]	15.0990
caster [gr]	9.0742
kingpin [gr]	9.8521
BT-long [mm]	21.3353
BT-lat [mm]	49.0818
m.crem. [mm]	15.0000
A.RUOTA EXT [gr]	8.0238
A.RUOTA INT [gr]	-8.7654
Dcamber/Druo[gr/gr]	-.1597
Dscuot /Druo[mm/gr]	.2015
Drapp /Druo[/gr]	.1442
Dpasso /Druo[mm/gr]	.8566
Dcam. /Druo[mm/gr]	.3724
D BTlon/Druo[mm/gr]	.6072
D BTlat/Druo[mm/gr]	-.1803
Dcaster/Druo[gr/gr]	.2189
Dkingp /Druo[gr/gr]	.0647

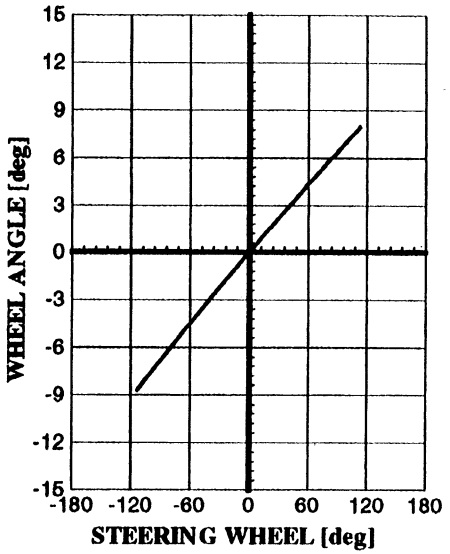

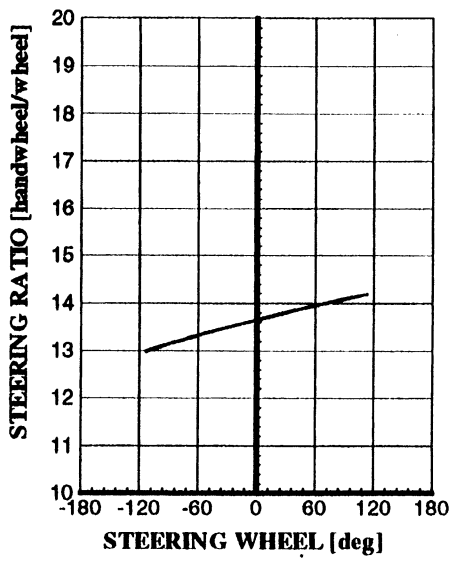

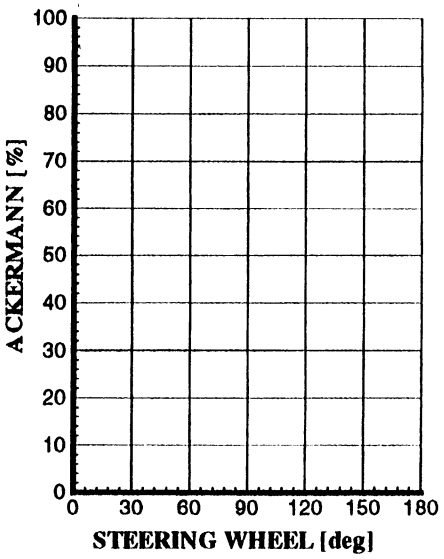

Figure 9b